Applied Surface Science 255 (2009) 4293–4297

Contents lists available at ScienceDirect

Applied Surface Science

journal homepage: www.elsevier.com/locate/apsusc

Influence of the substrate on ferroelectric properties of ⟨1 1 1⟩ oriented rhombohedral $Pb(Zr_{0.6}Ti_{0.4})O_3$ thin films

G. Leclerc, G. Poullain *, R. Bouregba, D. Chateigner

Laboratoire CRISMAT/CNRT-ENSICAEN, CNRS UMR 6508,Université de Caen Basse-Normandie, Boulevard Maréchal Juin, 14050 Caen Cedex, France

ARTICLE INFO

Article history:
Received 21 October 2008
Received in revised form 3 November 2008
Accepted 10 November 2008
Available online 21 November 2008

Keywords:
PZT thin films
Crystallographic orientation
Ferroelectricity
Ferroelectric domains

ABSTRACT

⟨1 1 1⟩-oriented $Pb(Zr_{0.6}Ti_{0.4})O_3$ thin films were elaborated in the same run by RF multitarget sputtering on $Si/SiO_2/TiO_2/Pt(1\,1\,1)$ and $LaAlO_3/Pt(1\,1\,1)$ substrates. PZT thin films were textured, exhibiting ⟨1 1 1⟩ fibre texture on silicon substrates whereas epitaxial relationships were found when grown on $LaAlO_3/Pt(1\,1\,1)$. On the latter substrate, values of spontaneous polarization and of dielectric permittivity were measured close to that calculated previously along the ⟨1 1 1⟩ direction of PZT rhombohedral single crystal. On the contrary, spontaneous polarization and dielectric permittivity measured on PZT thin films deposited on platinized silicon were found deviating from calculated values. These different electrical results are attributed to different ferroelectric domain configurations.

1. Introduction

Ferroelectric thin films have attracted much attention in the last years as they are promising candidates for integrated microelectronic devices [1,2]. Among them, the $Pb(Zr_xTi_{1-x})O_3$ (PZT) family is a good candidate for various devices. PZT is a perovskite-type ferroelectric material. Its crystal structure and physical properties depend strongly on the Ti/Zr ratio. At room temperature and for large Ti contents ($Ti/Zr > 52/48$) the crystal structure is tetragonal whereas it is rhombohedral for low Ti contents. These two crystallographic phases are separated by the so-called "morphotropic phase boundary" which is known to exhibit enhanced piezoelectric properties. Unfortunately, preparation of PZT single crystals has not been successful up to now, leading to a lack of information on the intrinsic anisotropy of the physical properties [3]. To overcome this difficulty, piezoelectric and dielectric coefficients related to different crystallographic directions were calculated by Du et al. [4]. Their results imply that oriented growth is needed for thin film device in order to take advantage of the best properties for a given application. Indeed, ferroelectric properties will be optimized when film growth is along the polar axis direction, whereas dielectric properties will be promoted when the polar axis is normal to the growth direction.

Several reports on the influence of PZT thin film orientation on ferroelectric properties confirmed the importance of such orientation monitoring during film preparation [5–7]. In a recent work, Kuwabara et al. [8] have shown that ferroelectric properties of epitaxially ⟨1 1 1⟩ oriented *tetragonal* PZT thin films were comparable to those of fiber-textured ones. Their results showed that the properties were not influenced by the strain state in the PZT thin film. The purpose of this work is to investigate the structural and electrical properties of *rhombohedral* PZT thin films deposited during the same run on two different substrates: $Si/SiO_2/TiO_2/Pt(1\,1\,1)$ and $LaAlO_3/Pt(1\,1\,1)$ (hereafter labelled as Pt/Si and Pt/LAO, respectively). This study describes the main results obtained from diffraction data and electrical characterizations, depending on the substrate, and examines them in the framework of the calculations made by Du et al. [4,9].

2. Experimental details

PZT films were prepared using RF multitarget sputtering system. Three metallic Pb, Zr, and Ti targets were used with magnetron cathodes. The stoechiometry is monitored by adjusting the RF power on each cathode. The composition studied in this paper is $Pb(Zr_{0.6}Ti_{0.4})O_3$ (PZT 60/40). The thickness of the films determined by SEM observations on cross section is 400 nm in all cases.

The substrates, (1 0 0)-oriented Si/SiO_2 and (1 0 0)-$LaAlO_3$ single crystal, are coated with a Pt sputtered layer of 150 nm and 100 nm in thickness, respectively. Note that the Si(1 0 0) substrate is covered by an amorphous silicon oxide layer of about 400 nm. In this case, a very thin TiO_2 layer (about 2 nm) was deposited before Pt layer deposition to ensure its adhesion and to

* Corresponding author.
E-mail address: gilles.poullain@ensicaen.fr (G. Poullain).

0169-4332/$ – see front matter © 2008 Elsevier B.V. All rights reserved.
doi:10.1016/j.apsusc.2008.11.033

promote its crystalline quality [10]. PZT thin films were sputtered during the same experimental run on both substrates, hence under exactly the same conditions. A very thin TiO_2 upper layer was also deposited prior to PZT sputtering in order to achieve in-situ crystallization and to promote growth along the ⟨1 1 1⟩ directions [11,12]. Sputtering conditions used to achieve a good orientation control were determined previously [10,11,13]. Energy dispersive spectroscopy (EDS) analyses performed on all the films showed no significant difference in cationic composition. Top Pt electrodes were deposited by sputtering and patterned with a lift-off process. They consist of squares of 235 μm in edge.

X-ray diffraction characterization in a θ–2θ reflection mode was carried out in order to get a first idea about films orientation. X-ray texture analysis was then carried out using a Huber 4-circle diffractometer equipped with a curved position detector (CPS 120-Inel) [14]. All X-ray measurements were performed with the Kα(Cu) wavelength, λ = 0.15418 nm. Pole figures were measured using 2.5° × 2.5° scan grid in tilt χ and azimuthal (φ) angles and processed using the Beartex software [15]. In what follows, we will always refer to the pseudocubic perovskite unit cell when talking about directions and planes of the rhombohedral PZT phase.

Ferroelectric measurements were performed at 1 kHz using a Radiant Technology Precision workstation. Dielectric response was obtained with an HP Agilent 4284A LCR meter.

3. Results and discussion

θ–2θ diffraction patterns of both samples on Pt/Si and Pt/LAO are shown in Fig. 1. The films are strongly oriented with {1 1 1} planes of Pt and PZT parallel to the substrate surface. The XRD patterns also reveal that the PZT film grown on Pt/Si contained a small volume fraction of ⟨1 1 0⟩ oriented grains. The lattice constant determined from the X-ray patterns is consistent with the rhombohedral phase (Please refer to Table 1). On the Pt/LAO substrate, a weak shift toward lower angles is detected for both ⟨1 1 1⟩-Pt and ⟨1 1 1⟩-PZT lines, when comparing to the Pt/Si substrate. This points out an in-plane compressive stress induced by the LAO substrate, and explains the increase of the lattice parameter of Pt and PZT when calculated from the out-of-plane d_{111} spacing (Table 1).

Table 1
Lattice parameters obtained from XRD data for PZT (60/40) thin films on Pt/Si and on Pt/LAO substrates.

Substrate	Film orientation	Pseudo-cubic unit cell parameter (Å)	
		Pt	PZT
TiO_x/Pt(1 1 1)/TiO_x/SiO_2/Si	⟨1 1 1⟩	a_p = 3.905	a_p = 4.08
TiO_x/Pt(1 1 1)/$LaAlO_3$(1 0 0)	⟨1 1 1⟩	a_p = 3.92	a_p = 4.105

On Pt/Si, both Pt and PZT layers exhibit a ⟨1 1 1⟩ fibre texture typical of the absence of epitaxial relationship with the substrate [16]. We do not expect a large contribution on the physical properties from the weak ⟨1 1 0⟩ component and neglect it. However, if the absence of epitaxy is clearly established for this film between the Pt bottom electrode and the substrate, one cannot prove this absence between PZT and Pt at the grain scale, because of the too large probed area compared to the crystallite size. Grain sizes in the range of 150–200 nm were determined by SEM and AFM observations. According to previous works [17,18], the fine grain sizes obtained on both substrates suggests that each individual grain contains probably only one ferroelectric domain.

The sample on Pt/LAO shows epitaxial relationships (Fig. 2) for Pt and PZT. The {1 1 6}-LAO pole figure (Fig. 2(a)) allows the determination of epitaxial relationships among LAO, Pt, and PZT (Table 2). The four poles from the LAO single crystal R-plane allow the location of the $[1\,1\,0]_p$ perovskite-like directions in the

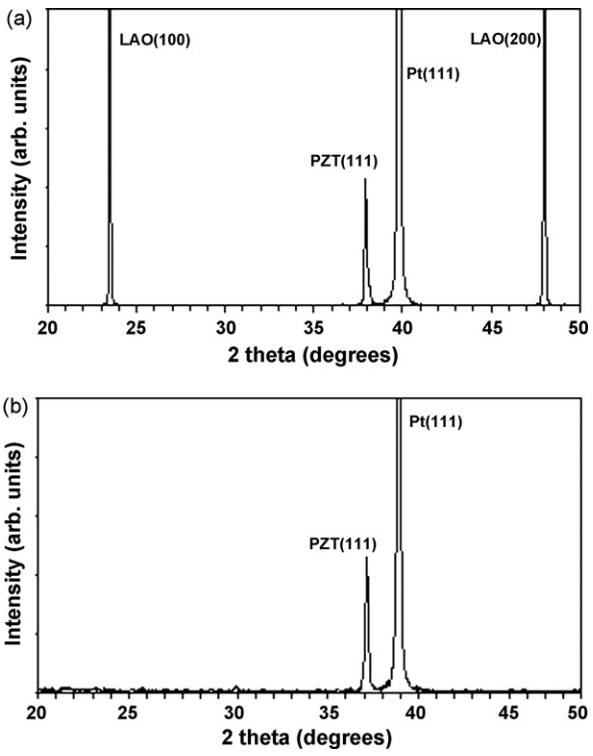

Fig. 1. XRD patterns of PZT 60/40 films: (a) on Pt/Si substrate and (b) on $LaAlO_3$/Pt substrate. The $\langle h\,k\,l\rangle_p$ indexation is related to the perovskite phase of PZT.

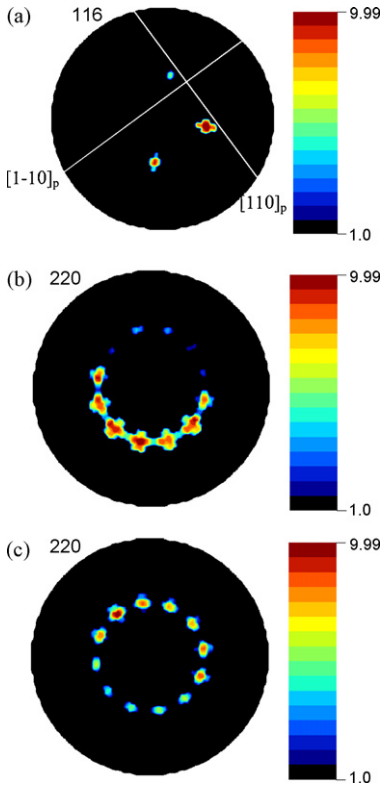

Fig. 2. Pole figures of the PZT 60/40 thin film deposited on $LaAlO_3$(1 0 0)/Pt(1 1 1). (a) {1 1 6}-LAO, (b) {2 2 0}-Pt, and (c) $\{2\,2\,0\}_p$-PZT pole figures. $[h\,k\,l]_p$ state for a pseudo-cubic indexing. Equal-area projections, logarithmic density scale.

Table 2
Crystallographic relationships between PZT thin films and substrates.

	Substrate	Electrode	Film	Relation
⊥	Si[1 0 0]/SiO_2	Pt[1 1 1]	PZT[1 1 1]	*Fiber*
⊥	LaAlO3[0 1 2]	Pt[1 1 1]	PZT[1 1 1]	*Epitaxial*
//	[1 1 0]	[1 1 0]	PZT[1 1 0]	

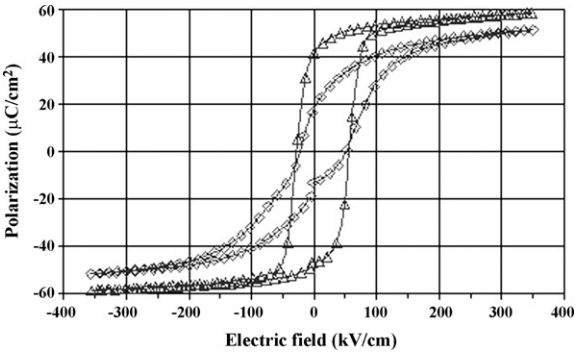

Fig. 3. Hysteresis loops of PZT 60/40 thin films on Pt/Si (diamond) and on $LaAlO_3$/Pt (triangle) substrates.

equatorial plane using simple crystallography. The {2 2 0}-Pt pole figure (Fig. 2(b)) shows 12 poles up to $\chi = 60^\circ$ whereas a perfect single crystal would exhibit only three for this ⟨1 1 1⟩ orientation. This means four epitaxial relationships are equivalently present in the Pt film. As for {1 1 6}-LAO, intensity variations between the poles are only due to the large scan grid used compared to the pole dispersion. This latter effect is less pronounced for {2 2 0}-PZT, indicating that this phase is slightly more distributed than Pt. The four equivalents are explained by the matching possibilities generated between the six ⟨1 1 0⟩ directions of Pt in the sample plane and the $\langle 1\,1\,0\rangle_p$-LAO directions. The same epitaxial components are stabilized in the PZT layer. Finally, the PZT thin film grown on Pt/LAO is textured. Furthermore, the whole PZT grains exhibit only four particular in-plane orientations. Then the PZT thin film on Pt/LAO may be considered as containing only four kinds of grains having epitaxial relationships with the substrate.

Hysteresis loops of both types of films are compared in Fig. 3 The PZT thin film on Pt/LAO substrate shows best ferroelectric properties: hysteresis loop with square-like shape and larger polarizations are obtained. However, the coercive fields are similar for both samples (around 40 kV/cm). As shown in Table 3, the

Table 3
Electrical properties of PZT thin films on Pt/Si and Pt/LAO and predicted value by Du et al. along the ⟨1 1 1⟩ direction.

PZT 60/40	P_r (μC/cm²)	E_c (kV/cm)	ε_r	tan δ
Calc. coefficients (Du et al.)	50	*X*	296	X
PZT on $LaAlO_3$/Pt(1 1 1)	46	42	390	0.027
PZT on Si/Pt(1 1 1)	19	38	790	0.024

remnant polarization obtained on LAO is close to the value of PZT 60/40 single crystals along the polar axis direction as calculated by Du et al. [4]. The dielectric permittivity values are consistent with those calculated, as well. On the other hand, both remnant polarization and dielectric permittivity measured on the PZT film deposited on the Pt/Si substrate deviate from the calculated values. Taylor and Damjanovic proposed that such a difference could be explained by an extrinsic contribution [6]. Indeed, strain imposed by the substrate in case of LAO/Pt may be at the origin of the observed differences, as explained in the following discussion.

Based on structural considerations, two ⟨1 1 1⟩-domain configurations can be expected. The four equivalent ⟨1 1 1⟩ axes in the pseudocubic cell are represented in Fig. 4(a). The rhombohedral ferroelectric structure can be seen as resulting from the lengthening of the paraelectric cubic phase along one of the four [1 1 1] directions. The specific [1 1 1] direction containing the polar axis will be labelled $[1\,1\,1]_{P\text{-axis}}$ in what follows. Then there exist three other ⟨1 1 1⟩ axes, which are non polar and tilted by 71° from $[1\,1\,1]_{P\text{-axis}}$. This suggests that optimized ferroelectric properties may be achieved if $[1\,1\,1]_{P\text{-axis}}$ is selected as the growth axis. This configuration is suspected to exist in the PZT sample deposited on the Pt/LAO substrate since large remnant polarizations were obtained. This implies that the Pt/LAO substrate imposes a peculiar arrangement of the PZT{1 1 1}-plane on Pt{1 1 1}, whereas the Pt/Si substrate does not. Epitaxial relationships found for the LAO sample show that the ⟨1 1 0⟩ directions of both PZT and Pt films are superimposed. Considering the rhombohedral structure, two kinds of ⟨1 1 0⟩ directions with different lengths are expected for each diamond face. Looking at the trigonal symmetry (Fig. 4(b)), the (1 1 1)-plane perpendicular to the $[1\,1\,1]_{P\text{-axis}}$ is the sole among all the {1 1 1} equivalents which intercepts the lattice cell by three short ⟨1 1 0⟩-segments. Now, the larger unit cell parameter of PZT measured normal to the Pt/LAO substrate surface (Table 1) implies in-plane compressive strains favouring short ⟨1 1 0⟩ segments parallel to the substrate plane. We can conclude that in this case the specific $[1\,1\,1]_{P\text{-axis}}$ crystallographic direction corresponds to

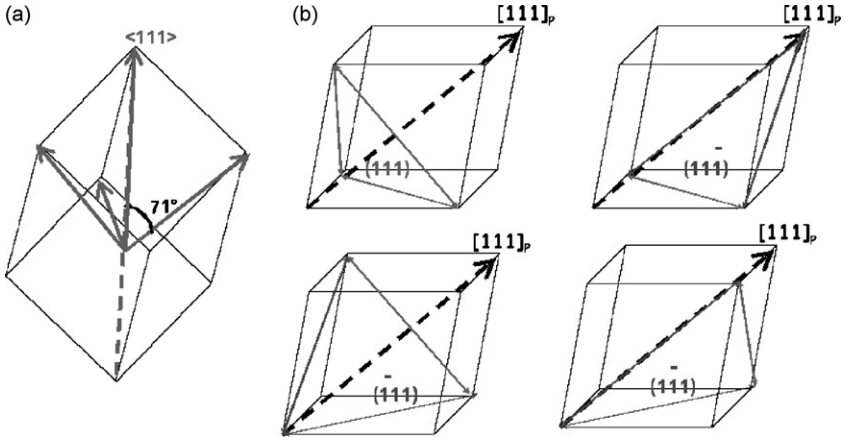

Fig. 4. (a) ⟨1 1 1⟩ directions in the pseudocubic cell for a cell oriented along the [1 1 1] direction. The rhombohedral distortion implies the stretching of the [1 1 1] direction which is defined as the polar axis and labelled $[1\,1\,1]_{P\text{-axis}}$ in the text.
(b) {1 1 1} planes are defined by three ⟨1 1 0⟩ directions. In the rhombohedral cell, the (1 1 1) plane normal to the [1 1 1] polar axis contains three short ⟨1 1 0⟩ distances in the lattice cell contrary to the other {1 1 1} planes that present also long ⟨1 1 0⟩ distances.

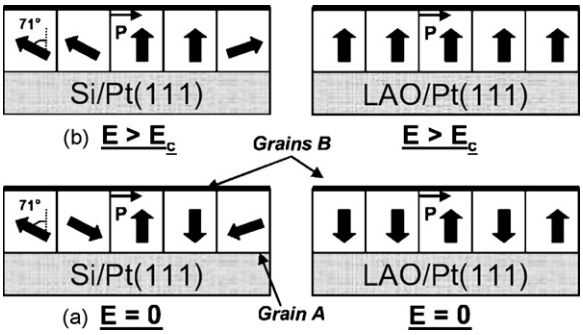

Fig. 5. Schematic domain configurations of PZT thin films deposited on Pt/Si and on Pt/LAO. Domain configuration is expected to be random on Pt/Si substrate while 180°-domains normal to the film surface may be imposed by the substrate on Pt/LAO.

the growth axis. Dealing with the PZT sample on Pt/Si, it is suspected that no specific relationships are imposed by Si on Pt since no epitaxial growth was detected. Thus the growth axis for the PZT layer on Pt/Si should be a random mixture of all the ⟨1 1 1⟩ directions.

As a consequence, the fact that the properties of PZT films on Pt/LAO are close to that of single crystals can be explained in terms of different domain configurations. Indeed, for PZT films on Pt/LAO, the domain configuration consists probably of 180° switching domains perpendicular to the electrode plane (see grain B in Fig. 5). Then, for an applied electric field a bit larger than E_c, most domains are likely to be switched on Pt/LAO. This is consistent with the large value of the remnant polarization and also with the square-like shape of the hysteresis loop. For PZT films on Pt/Si however, the tilt of the hysteresis cycle may be attributed to the 180° switching domains from grains which polarization axis are tilted by 71° from the [1 1 1] growth direction. It may be considered that a random distribution of polar axis exists in this sample, and that the ⟨1 1 1⟩ growth direction is a mixture of $\langle 1\,1\,1\rangle_{P\text{-axis}}$ and of the three other ⟨1 1 1⟩ non polar directions. So, 75% of the grains are expected to grow along a non polar axis, in such a way that for these grains, the $[1\,1\,1]_{P\text{-axis}}$ is tilted by 71° from the normal of the substrate surface (see grain A in Fig. 5). When applying an electric field to these tilted grains, the polarization reversal is obtained through the switching of the polarization by 180° from 109° domain to 71° domain (compare grain A in Fig. 5 (a) and (b)). This is consistent with previous works of Xu et al. [17] and Kim et al. [19] who showed that 180° switching domains only contribute to the ferroelectric properties of PZT thin films. This switching mode requires large electric field ($E > E_c$) and the contribution to the polarization along the normal is lower. Note that similar E_c on Pt/LAO and Pt/Si samples may be a consequence of this common 180° switching behaviour. The contribution of the domain walls in this configuration is also responsible for the anomalous increase of the dielectric permittivity [6,19], compared to the calculated value [4].

The different values of the remnant polarization obtained for the films deposited on both types of substrates are found to be rather consistent with the tilt of the grains on Pt/Si. Indeed, as the remnant polarization of the film deposited on Pt/LAO is 46 μC/cm^2 (Table 3), one expects, with 75% of the grains tilted by 71°, an average value of $0.25 \times 46 + 0.75 \times 46 \times \cos(71^\circ) = 22.7$ μC/cm^2. This is in good agreement with the experimental value of around 19 μC/cm^2 measured on the film deposited on Pt/Si. Taking into account that this film also contains other textural components like ⟨1 1 0⟩, the difference of around 4 μC/cm^2 between calculated and experimental values may be explained by considering that 88% of the grains have their polar axis 71° or 109° away from the normal to the film surface. The contribution of the few ⟨1 1 0⟩ oriented grains may also partially explain the lower value of saturation polarization that was obtained on Pt/Si. We cannot also totally avoid that some domain wall pinning occurs that may explain the slight reduction of maximum polarisation, but as the coercive field is the same on both substrates, domain pinning cannot be the main origin of the large difference observed for remnant polarization.

Finally, the stress imposed in-plane by the LAO substrate on the PZT film can be calculated. The strain ε_3 along the normal of the film plane is determined from the measured cell parameters, $\varepsilon_3 = (a_p^{PZT/LAO} - a_p^{PZT/Si})/a_p^{PZT/Si} = 6.10^{-3}$. Within the linear elasticity hypotheses, and considering that no shear stress is applied on the film, the stress components σ_i (i = 3–6) are all equal to zero. Since the Pt/LAO substrate impose $\sigma_1 = \sigma_2$ in the film plane, one can obtain the in-plane deformation $\varepsilon_1 = \varepsilon_2$ using a biaxial stress state for a single crystal [20]: $\varepsilon_1 = -c_{33}/c_{31} + c_{32}\ \varepsilon_3$, and $\sigma_1 = (c_{11} + c_{12})\ \varepsilon_1 + c_{13}\ \ \varepsilon_3 = 1.4$ GPa, with $c_{11} = 135$ GPa, $c_{33} = 113$ GPa, $c_{12} = 67.9$ GPa, $c_{13} = c_{23} = 68.1$ GPa. This very high value of residual stress ($\sigma_1 = 1.4$ GPa) helps promoting centro-symetric properties in the sample plane, in favour of the perpendicular development of the polarization.

4. Conclusion

This work shows that contrary to the case of tetragonal PZT thin films studied by Kuwabara et al. [8], electrical properties of rhombohedral PZT thin films are strongly influenced by the strain state in the films. Ferroelectric properties of rhombohedral PZT thin films may be optimized by monitoring the strain imposed by the substrate, which strongly affects the domains configuration. In this paper, we showed that the growth of the film along the polar axis can be favoured by the stress induced by the substrate. This was the case for PZT 60/40 films with [1 1 1] preferred orientation deposited on $LaAlO_3$/Pt(1 1 1) substrate. Most of the grains are then 180° ferroelectric domains normal to the film surface, and the ferroelectric properties were optimized. On the contrary, similar PZT thin films deposited on Pt/Si(1 1 1) present weaker ferroelectric characteristics but enhanced dielectric permittivity. In this case, the tilt of 180°-domains by 71° from the normal of the substrate due to the non-preferential $[1\,1\,1]_{P\text{-axis}}$ growth leads to lower remnant polarizations. On the other hand, the increase of dielectric permittivity may be explained by this tilt of the ferroelectric domains, through a domain wall contribution to the permittivity.

Acknowledgments

The authors would like to thank Dr. J. Ricote (Instituto de Ciencia de Materiales de Madrid, CSIC, Cantoblanco, E-28049 Madrid, Spain) for helpful discussions. This work was supported by the CNRS-CSIC cooperation program (2004FR0030). The Région Basse-Normandie is warmly acknowledged for financially supporting GL's PhD and the X-ray texture instrument.

References

[1] J.F. Scott, C.A. Paz de Araujo, Science 246 (1989) 1400.
[2] C.H. Ahn, K.M. Rabe, J.-M. Triscone, Science 303 (2004) 488.
[3] B. Noheda, Curr. Opin. Solid State Mater. Sci. 6 (2002) 27.
[4] X. Du, U. Belegundu, K. Uchino, Jpn. J. Appl. Phys. 36 (1997) 5580.
[5] G. Le Rhun, G. Poullain, R. Bouregba, G. Leclerc, J. Eur. Ceram. Soc. 25 (2005) 2281.
[6] D.V. Taylor, D. Damjanovic, Appl. Phys. Lett. 76 (2000) 1615.
[7] J. Hong, H.W. Song, H.C. Lee, W.J. Lee, K. No, J. Appl. Phys. 90 (2001 1962).
[8] H. Kuwabara, N. Menou, H. Funakubo, Appl. Phys. Lett. 90 (2007) 222901.
[9] X. Du, J. Zheng, U. Belegundu, K. Uchino, Appl. Phys. Lett. 72 (1998) 2421.
[10] B. Vilquin, G. Le Rhun, R. Bouregba, G. Poullain, H. Murray, Appl. Surf. Sci. 195 (2002) 63.
[11] R. Bouregba, G. Poullain, B. Vilquin, H. Murray, Mater. Res. Bull. 35 (2000) 1381.
[12] B. Vilquin, R. Bouregba, G. Poullain, M. Hervieu, H. Murray, Eur. Phys. J. Appl. 15 (2001) 153.

[13] G. Leclerc, B. Domenges, G. Poullain, R. Bouregba, Appl. Surf. Sci. 253 (2006) 1143.
[14] M. Morales, D. Chateigner, L. Lutterotti, J. Ricote, Mat. Sci. Forum 408 (2002) 113.
[15] H.R. Wenk, S. Matthies, J. Donovan, D. Chateigner, J. Appl. Crystallogr. 31 (1998) 262.
[16] D. Chateigner, H.R. Wenk, A. Patel, M. Todd, D.J. Barber, Int. Ferroelectr. 19 (1998) 121.
[17] F. Xu, S. Trolier-McKinstry, W. Ren, B. Xu, Z.-L. Xie, K.J. Hemker, J. Appl. Phys. 89 (2001) 1336.
[18] N. Floquet, J. Hector, P. Gaucher, J. Appl. Phys. 84 (1998) 3815.
[19] D.-J. Kim, J.-P. Maria, A.I. Kingon, S.K. Streiffer, J. Appl. Phys. 93 (2003) 5568.
[20] V. Hank, Structural and Residual Stress Analysis by Non Destructive Methods: Evaluation, Application, Assessment, Elsevier, Amsterdam, 1997.